ACS APPLIED MATERIALS & INTERFACES

Research Article

www.acsami.org

Vertical Graphene Spin Valves Based on $La_{2/3}Sr_{1/3}MnO_3$ Electrodes

Feng Li,* Tian Li, and Xinyi Guo

High Magnetic Field Laboratory, Chinese Academy of Sciences, Hefei 230031, China

ABSTRACT: We report the fabrication of the $La_{2/3}Sr_{1/3}MnO_3$ (LSMO)/graphene/Co sandwich structures employing single-layer graphene as the interlayer. Appreciable negative spin valve signals were observed from room temperature to 5 K. We find that the devices demonstrate nonlinear current−voltage (I−V) characteristics around room temperature, indicating that the tunneling effect is dominated rather than the Ohmic property. However, I−V curves exhibit evident linear behavior at low temperatures, which reveal the Ohmic characteristic. The vertical graphene spin valves using LSMO electrode have potential application in memory storage and logic operation.

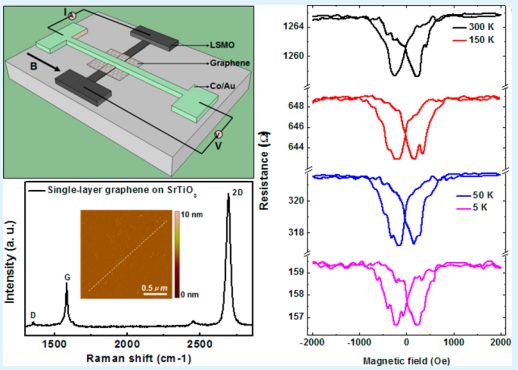

KEYWORDS: *spintronics, magnetoresistance, graphene, chemical vapor deposition, spin-dependent transport*

INTRODUCTION

Recently, carbon-based materials have became a promising candidate material in spintronic research and applications, motivated by their long spin-relaxation lifetimes due to the weak spin−orbit interaction and hyperfine interaction.[1−9] Graphene is a typical carbon-based material, which is a strictly two-dimensional (2D) material with honeycomb carbon lattice, and was investigated broadly on the extraordinary in-plane charge carrier mobility and long mean free path, and there has been extensive research interest in the relaxation mechanisms and spin transport properties in graphene.[10−12] Therefore, because of the fascinating advantages of high carrier mobility and long spin lifetime, most the researchers have begun to participate in the graphene spintronic research. Especially long spin diffusion length of about a few micrometers in graphene have been clearly observed in the devices using both two and four terminal geometries.[13−15] Several groups have demonstrated graphene lateral spin-valve structures with long spin lifetimes and diffusion lengths.[15,16] Apart from the traditional planar transport graphene devices, current perpendicular to graphene plane configuration is another vital research direction for graphene application.[17] Injection of highly (75%) spin-polarized electrons into 17 nm thick graphite nanostructures, which is the parent compound of graphene, perpendicular to the layer plane was achieved successfully employing scanning tunneling microscopy based techniques.[18] In the structure which used graphene and 2 nm Au layer as the interlayer and employed the perm alloy as the bottom and top ferromagnetic electrodes, an enhanced magnetoresistance (MR) effect compared to a simple stack without the graphene layer was obtained.[19] The magnetic tunnel junctions employed graphene as the tunnel barrier, with a structure of perm alloy/monolayer graphene/Co that has been fabricated successfully and studied deeply.[20] The nonlinear current−voltage (I−V) behaviors and the analysis of zero bias resistance (ZBR) reveal that graphene serves effectively as a tunnel barrier for the spin transport perpendicular to the device plane. However, compared with the tunneling barrier, the results that the graphene acted not as tunnel spacer but rather as conducting interlayer were also considerably reported,[21−23] and the graphene spin valves with ohmic contact may have many advantages for the application. Thus, the function of graphene, whether in the tunneling barrier or conducting interlayer, in the spin valve structure has been becoming a confusing debate. Therefore, this research issue merits further deep investigation.

In this paper, we report the vertical graphene spin valves with current perpendicular to plane configuration by inserting single-layer graphene between the highly spin polarized LSMO and Co ferromagnetic electrodes. It is found that the devices demonstrate linear I−V curves at temperatures from low temperature to about 225 K, indicating that Ohmic property is dominant, but at the temperatures from nearly 225 K to room temperature, the I−V curves show the nonlinear property, which indicates the tunneling effect. Evident spin valve signals are observed in devices with single-layer graphene interlayer at both low temperature and room temperature. Our results will further expand the area of graphene applications to memory storage, logic operation, and even more complex graphene based nanoscale devices.

EXPERIMENTAL SECTION

Device Fabrication. The device structure is shown schematically in Figure 1a. The 60 nm thick and about 0.05 mm wide LSMO films, which is the half-metallic ferromagnet with nearly 100 % spin polarization and is also very stable, were deposited on $SrTiO_3$ (STO)

Received: November 1, 2013
Accepted: January 3, 2014
Published: January 3, 2014

   dx.doi.org/10.1021/am404866r | ACS Appl. Mater. Interfaces 2014, 6, 1187−1192

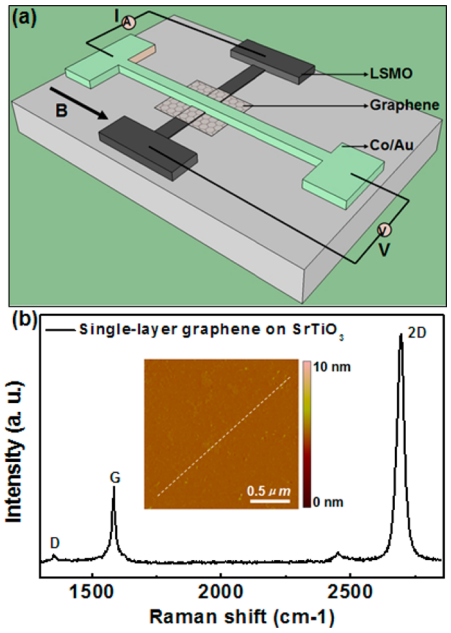

Figure 1. (a) Schematic diagram of our vertical spin valve device with a $SrTiO_3$ substrate/$La_{2/3}Sr_{1/3}MnO_3$/graphene/Co/Au. (b) Raman spectra (515.2 nm wavelength) for single-layer graphene film after transfer to the $La_{2/3}Sr_{1/3}MnO_3$ electrode; the inset show the atomic force microscopy (AFM) image of single-layer graphene transferred onto the LSMO surface.

⟨100⟩ substrates using pulsed laser deposition method through a shadow mask. Single-layer graphene films studied in this experiment were grown on 25 μm thick Cu foils using the low-pressure chemical vapor deposition (CVD) method in a tube furnace. The Cu substrate, a polycrystalline Cu foil cut in 3.0 × 1.5 cm^2 squares, was heated to 1000 °C at a heating rate of 2 °C/s in a vacuum with a base pressure of ~10 Torr. During the grown progress, CH_4 gas with a flow rate of 50 standard cubic centimeters per minute (sccm) and H_2 gas (30 sccm) as the sources were introduced into the chamber. Then the temperature of the Cu substrate was stabilized at 1000 °C for 30 min. Subsequently the Cu substrate was cooled rapidly to room temperature.

The graphene films grown on Cu foil were transferred onto a STO substrate with LSMO electrode using a wet transfer method. Before the graphene films were wet-etched, poly(methyl methacrylate) (PMMA) was spin coated onto the surface of graphene films, and then the graphene films with PMMA resist were baked at 180 °C for 10 min. The purpose of the PMMA spin coating onto graphene films is to protect the graphene films from cracking and breaking during the transfer process. The bottom Cu foil was removed by dissolving in the solution of ammonium persulfate (APS) ($(NH_4)_2S_2O_8$), and the PMMA membrane was washed with deionized water. The resulting graphene films and attached PMMA membrane were transferred onto the STO substrate with the prefabricated LSMO electrode. The residual PMMA film was dissolved and removed in the acetone solution.[20,21]

Finally, the 10 nm thick Co film was thermally evaporated as the top ferromagnetic electrode and subsequently capped with a 30-nm Au protection layer using a shadow mask. The cross-bar junction area was about 50×10 μm^2. After investigation of the characteristics of graphene, the oxygen plasma etching was employed to remove the unnecessary graphene (apart from that at the designated junctions).

In this paper, we have prepared 10 devices using the same fabrication processing. And all those 10 devices were selected to be characterized and measured. We found that about 60% of these showed the obvious spin valve behavior and other properties depicted in the Results and Discussion, while the others were shortened, which may be caused by the unseen processing related issues.

Device Characterization and Measurement Setup. A Raman spectrometer was used to characterize the single-layer graphene samples. The morphology of the single-layer graphene film was characterized with a Veeco MultiMode (nanoscope V) AFM in tapping mode. The MR values of the devices were measured in a Quantum Design Physical Property Measurement System (PPMS) under an external in-plane magnetic field from room temperature (300 K) to 5 K using the standard four-probe method. Current-voltage (I–V) measurements were performed using a Keithley 2612 source measure unit, with the positive pole connected to the LSMO electrode.

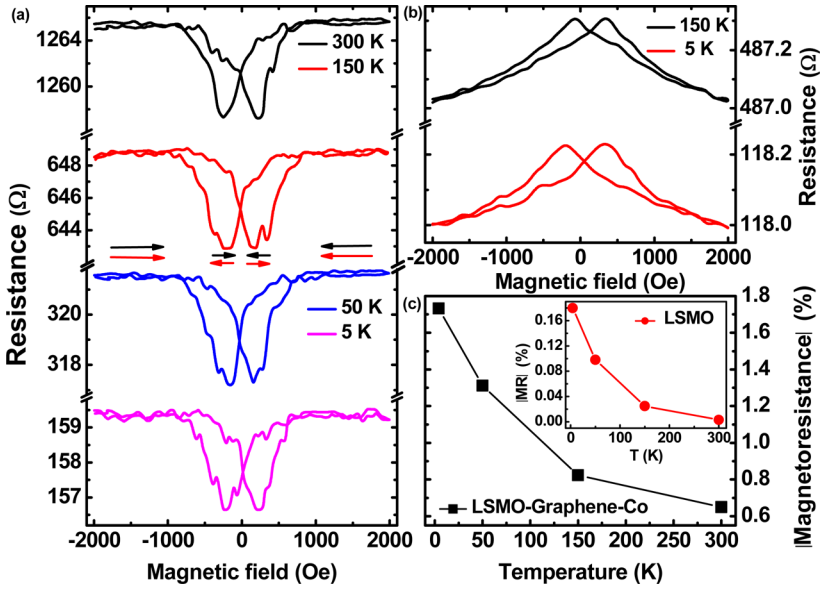

Figure 2. (a) Magnetoresistance curves of our vertical spin valve device measured at different temperatures of 300 K, 150 K, 50 K, and 5 K. (b) Field dependence of magnetoresistance curves for $La_{2/3}Sr_{1/3}MnO_3$ measured at 150 K and 5 K. (c) Temperature dependence of the absolute value of the magnetoresistance ratio of our vertical spin valve device. The inset shows the temperature dependence of the magnetoresistance ratio of the $La_{2/3}Sr_{1/3}MnO_3$ electrode.

RESULTS AND DISCUSSION

Figure 1a shows the schematic device structure and the measurement configuration of a graphene spin valve consisting of a bottom LSMO electrode, top Co electrode, and single-layer graphene interlayer. The LSMO electrode was chosen as the bottom electrode in our SV devices, because LSMO is the half-metallic oxide ferromagnetic material which exhibits nearly 100% spin polarization at low temperature.[3] Moreover, as LSMO is a typical oxide, unlike metallic ferromagnetic materials such as cobalt, nickel, iron, and other alloys, it displays environmental stability. While current flows from LSMO to Co through the graphene interface, voltage is measured between LSMO and Co. As show in Figure 1a, the in-plane magnetic field (H) was applied and aligned with the long Co electrode axis, the magnetization emerging parallel to the current flow in it, and that is the magnetization perpendicular to the current flow in the bottom LSMO electrode. The LSMO ferromagnetic electrode and Co ferromagnetic electrode show the different switching fields of magnetization. Therefore, the magnetization alignments can be made parallel or anti-parallel by sweeping the external magnetic field.

The graphene interlayer in our spin valve device is a single-layer graphene. Figure 1b shows the Raman spectra measured for the graphene interlayer, where the intensity ratio between 2D and G band peaks is $I_{2D}/I_G \approx 2.8$ for single-layer. A ratio higher than 2 confirms that the interlayer graphene is a single layer.[24,25] The 2D peak was found at 2676 cm^{-1} for the single-layer graphene. However, the low intensity of the D band peak indicates the good quality of our single-layer graphene. Furthermore, we have also performed the AFM measurements to find out the surface morphology of the single-layer graphene on the LSMO surface. The inset of Figure 1b shows the typical surface topographic image of single-layer graphene transferred onto the LSMO surface with the scanning size 2 μm ×2 μm. The film displays a homogeneous surface, and the surface morphology of the film is very smooth. The root mean squared (RMS) roughness is 0.09 ± 0.002 nm. The RMS roughness is independent of single-layer graphene thicknesses (about 0.4 nm). Due to the low roughness and high smoothness, the possible presence of the pinholes within the single-layer graphene interlayer could be excluded. After examining the graphene by Raman spectroscopy and AFM we removed the unnecessary graphene part which was not located underneath the Co electrode by oxygen plasma etching. This removal of unnecessary graphene was essential to prevent flowing bypass current outside the junction.

Figure 2a shows the typical MR curves for the vertical graphene spin valve devices composed of the single-layer graphene measured at 300 K, 150 K, 50 K, and 5 K, respectively. First of all, it is worthy to be noted definitely that the junction resistance of the devices decreases monotonously with decreasing measured temperature. For the graphene SV device measured at 300 K, the resistance is more than 1000 Ω, while for the device measured at 5 K, its resistance exhibits less than 200 Ω. The above result is somewhat different from the previous research results on the organic spin valve devices.[1−9] We speculate preliminarily that the occurrence of the above result may originate from the fact that the single-layer graphene was used as the interlayer in our spin valve devices. In addition, the figure also shows that the magnitude of the MR signal decreases with the increasing measured temperature. The MR values are defined by the expression $MR(\%) = 100 \times (R_{AP} - R_P)/R_P$, where R_{AP} and R_P are the resistances of the anti-parallel and parallel magnetization configurations of two electrodes, respectively. The MR ratios of our vertical graphene SV devices, calculated based on the resistances of the device which were measured at different temperatures and are shown in Figure 2a, are 0.63%, 0.82%, 1.31%, and 1.73% measured at 300 K, 150 K, 50 K, and 5 K, respectively. Furthermore, we can see that all the devices show a typical negative MR loop, which is in accordance with the previous report in the organic spin valve devices employing the LSMO and Co as the electrode,[3−5,8,9] but is different from the positive MR curves of the vertical graphene SV devices in the previous research.[20−23] Moreover, we obtained the obvious MR ratio of about 0.63% at room temperature (300 K). Actually, room temperature MR signals were also obtained in the previous reports on the vertical graphene SV devices,[20−23] in which the ferromagnetic metals or ferromagnetic alloys were used as the devices electrodes. Despite the fact that few room temperature MR effects have been achieved in the organic SV devices in which the LSMO was used as the electrode, recent reports show that appreciable room temperature MR signals were obtained in the organic SV devices that employed LSMO as the electrodes[8,9] and further certify that the MR temperature dependence of the LSMO based organic SVs mainly originate from the decrease of spin polarization of the LSMO electrode.[9]

The junction resistances of our prepared vertical graphene SV devices present the similar order of magnitude as the resistance of the LSMO electrode. And we know that the LSMO film itself possesses the properties of the magneto-resistance effect, including the normal magnetoresistance effect (NMR) and the anisotropic magnetoresistance effect (AMR). The NMR defined here is $\Delta\rho/\rho = (\rho_H - \rho_0)/\rho_0$, where the ρ_H and ρ_0 are the resistances with and without a field of H. Meanwhile, the AMR effect is also usually discovered in the Co films. Therefore, the origin for the large MR effect in our graphene SV devices measured at the different temperatures *may* be the MR effect of the bottom LSMO electrode or the AMR effect of the top Co electrode rather than the spin valve effect of the devices themselves. In order to further clarify this issue on the origin of MR effect in our devices, we have performed the MR measurement of the LSMO electrode individually while the magnetic field is swept in the same direction as in the MR measurement of our graphene SV devices, which is the magnetization perpendicular to the current flow in the LSMO film. Figure 2b shows the MR curves for the LSMO film measured at 150 K and 5 K. Comparing Figure 2a with Figure 2b, we can find that the resistances of the LSMO electrode measured at different temperatures are a little smaller than the junction resistances of the graphene SV device measured at the corresponding temperatures, but we also find that the resistances of the LSMO electrode and the junction resistances of the device have the similar order of the resistance magnitude. This phenomenon described above increases our suspicious on the issue that the origin of the MR effect of the graphene SV devices may be from the LSMO electrode. However, from Figure 2b we can further find that the LSMO electrode really shows the MR effect, but it is noteworthy that the MR signals measured at 150 K and 5 K are both positive, while the negative MR effect was found in our graphene SV device, which indicates that the MR effect of the graphene SV device should not arise from the MR effect, including the NMR effect and the AMR effect, of the LSMO electrode. Additionally, we have also performed the AMR measurement of the Co film,

capped with Au film as in our graphene SV structure, individually. The magnetic field is aligned with the long Co film axis making the magnetization parallel to the current flow in the Co film, which is also as the MR measurement in the graphene SV devices. We have not observed the increase of the resistance of the Co film with the magnetic field, which is caused by the effect of the AMR in the Co film. It is more likely because the Co film is shunted by the gold capping layer.[18] Furthermore, since the fabricated graphene SV devices show a junction resistance larger than that of the Co electrode, the MR signal in the graphene SV device should also not be associated with the AMR effect in the Co electrode.

In order to further investigate the origin of the MR effect in our vertical graphene SV device, we measured the MR ratios of the LSMO electrode at different temperatures, and we also compared them with the MR values of the device. The main panel of Figure 2c shows that the magnitude of the MR signal of the graphene SV device decreases with increasing temperatures, which is in agreement with results reported by others on the organic SV devices.[1−9] We find that our device displayed about 0.63% MR effect when the device was measured at room temperature. The inset of Figure 2c shows that the magnitude of the MR value of the LSMO electrode also decreases with increasing temperatures, which is similar with that of the graphene SV device. But we can also find that the MR ratios of the LSMO electrode measured at different temperatures are much less than those of the graphene SV devices measured at the corresponding temperatures. This further reveals that the MR effect of our graphene spin valve devices do not arise from the MR effect of the LSMO electrode but the spin valve effect of the device itself.

To gain deeper insight into the mechanism of the MR effect in our vertical SV devices with single-layer graphene interlayer measured at different temperatures, current−voltage ($I-V$) characteristics were measured at different temperatures and were studied, as shown in Figure 3. We can find that the $I-V$ characteristics show the strictly linear behavior at the measured temperatures from 175 K to 5 K, which suggest initially that the contact between graphene and both LSMO electrode and Co electrode are perfect Ohmic, and the graphene interlayer works as a conducting thin film in our device from 175 K to 5 K. Moreover, the $I-V$ curves are largely temperature dependent at the measured temperature from 175 K to 5 K, and the junction resistance of the SV device decreases as decreasing temperature in the above measured temperature scope, which shows that the transport mechanism in the vertical direction of single-layer graphene is metallic. Here, the Ohmic property of the transport through the graphene layer in our device is different from the previous literatures which have reported a tunneling transport of the $Ni_{0.9}Fe_{0.1}$/graphene/Co device[20] but is similar with the previous reports of the conducting properties in the Co/graphene/Co structures and NiFe/graphene/NiFe structures.[21−23] The work function of graphene is in the range of 4.5−4.8 eV, and the work functions of LSMO, Co, and Ni are about 4.8 eV, 4.9 eV, and 5.1 eV, respectively. Because the work function difference between graphene and both the LSMO and Co is much smaller than that between graphene and Ni, our devices may demonstrate Ohmic property rather than tunneling transport.

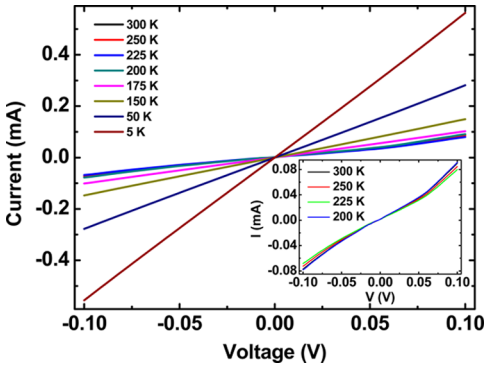

Figure 3. Typical current−voltage ($I-V$) curves at different temperatures for the $La_{2/3}Sr_{1/3}MnO_3$/graphene/Co spin valve device with the single-layer graphene. The inset shows $I-V$ characteristics for our graphene spin valve at the temperatures of 300 K, 250 K, 225 K, and 200 K.

However, when our SV devices were measured at the temperature from nearly 200 K to room temperature, we can find that the $I-V$ characteristics display the nonlinear behavior at this temperature scope. In order to show the non-linear $I-V$ behavior clearly and intuitively at the measured temperatures from 200 K to 300 K, we magnify the above corresponding part, which was shown in the inset of Figure 3. We can find clearly that the $I-V$ curves (measured at 200 K, 225 K, 250 K, and 300 K, respectively) are nonlinear and symmetric. Furthermore, the inset of Figure 3 also shows that $I-V$ curves are weakly non-linear and are almost temperature independent. All of the above experimental characteristics and the corresponding analysis indicate the evident characteristic of a metal/insulator/metal tunnel junction when our graphene SV devices were measured at temperatures from 200 K to the room temperature.[26] Although the bottom electrode was exposed in the air for a little while before the graphene was transferred onto it, the bottom electrode in our vertical graphene SV devices is the LSMO thin film which is the half-metallic ferromagnetic oxide and is very stable against oxidation. So during the devices fabrication, any oxidation of the bottom electrode may not produce the so-called thin oxidized layer, which may act as the tunneling interlayer and occur in the spin valve devices employing the ferromagnetic metal as the bottom electrode.

On the basis of the above $I-V$ characteristics measurement and the corresponding analysis, together with the observation of MR features in the graphene SV device, we speculate initially that the graphene acts as the conducting interlayer in our graphene SV devices at the measured temperatures from 175 K to 5 K, while at the measured temperatures from 200 K to 300 K the graphene mainly works as the tunnel barrier. It should be an unintelligible puzzle why the function of the graphene interlayer is so different in the same graphene SV device which was just measured at the different temperatures.

However, it should be pointed out that in the pervious literatures on the vertical graphene spin valves the bottom electrode and the top electrode are mainly the same ferromagnetic metallic electrode and different ferromagnetic metallic electrode,[20−23] and the bottom electrode and the top electrode usually have the same or similar electricity conductivity, while in our fabricated vertical graphene SV devices, the bottom electrode and the top electrode are the different ferromagnetic materials. Generally, the LSMO thin film is the ferromagnetic half-metallic oxide, while the top Co electrode is the ferromagnetic metal, and they usually have different electricity conductivity accordingly. So we conjecture

preliminary that the conductivity mismatch may cause the different functions of graphene interlayer in the device measured at different temperatures. Such issue merits further investigation.

On the basis of the above analysis, and with a view to more insight into the origin for the large value of MR ratio at the room temperature and the function of the graphene in our SV devices, we have performed the measurements of the temperature dependence of the resistance of the bottom LSMO electrode and that of the graphene spin valve device. Figure 4a shows the temperature dependence of the resistance

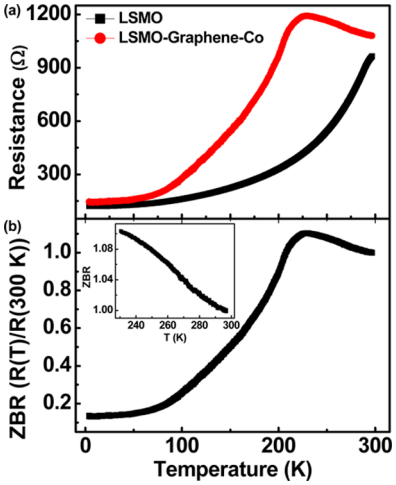

Figure 4. (a) Temperature dependence of the resistance of the $La_{2/3}Sr_{1/3}MnO_3$ electrode and the vertical graphene spin valve device. (b) Zero bias resistance (ZBR) vs temperature for the graphene spin valve device. The inset shows the magnification of the ZBR at the temperatures from 225 K to 300 K.

of the LSMO electrode and our vertical spin valve device. The resistances of the device in Figure 4a correspond with measured results which are shown in Figure 2a. It is also shown from Figure 4a that the magnitude of resistance of the device and that of the LSMO electrode are always in the same order at the same measurement temperature from 5 K to 300 K. Meanwhile, the resistances of the LSMO electrode are always a little smaller then that of the graphene SV device. The temperature dependence of resistance of the LSMO electrode shows that the resistance of the LSMO electrode exhibits strong temperature dependence and increases with increasing temperature. The sharpness of the transition demonstrates the high quality of our sample, which is consistent with the previous experiments on the LSMO film,[27] in which the metal−insulator (M−I) transition occurred at about 320 K. While for the graphene spin valve device, we can find that at the temperature from 5 K to 225 K the resistance increases with increasing temperature moderately at first and then increases very sharply; this is similar with the trend of temperature dependence of the resistance of the LSMO electrode. However, in the measured temperature range between 225 K and 300 K, we can find that the resistance of the SV device decreases with the increasing measured temperature moderately. This is a fascinating physical phenomenon, and this can also further substantiate the assumption in the above paragraph that the function of the graphene in our SV device from low temperature to 225 K mainly works as the conducting interlayer, while from 225 K to the room temperature, the graphene mainly acts as the tunnel barrier in the device.

Furthermore, we then have a further analysis on the resistance of the graphene spin valve device to find out the role of graphene in our device. Figure 4b shows the typical zero bias resistance (ZBR) of our vertical graphene spin valve device, which was defined as $R(T)/R$ (300 K). It is shown clearly that the resistance of the device increases sharply with the measured temperature from low temperature to 225 K, while at the temperature from 225 K to room temperature, the resistance of the device decreases with the increasing temperature modestly. It confirms plenty that the graphene interlayer works as the conducing interlayer from 5 K to 225 K and the tunnel barrier from 225 K to room temperature.

CONCLUSION

In summary, we have prepared the vertical graphene SV devices with the single-layer graphene spacer using LSMO as the bottom electrode and observed the negative magnetoresistance effect. The interesting larger value of the MR ratio was observed in our device at room temperature, which provides practical value for the application. Detailed MR curves and $I-V$ characterizations of the devices indicate a transition of the role of graphene from conducting spacer, at the temperatures from 5 K to 225 K, into tunneling barrier measured at the temperatures from 225 K to room temperature. The $R-T$ measurements of the device and the LSMO electrode further illustrate the function transition of the graphene interlayer mainly originating from different conductivities of the bottom electrode and the top electrode.

AUTHOR INFORMATION

Corresponding Author

*E-mail: lfeng99@mail.ustc.edu.cn.

Notes

The authors declare no competing financial interest.

REFERENCES

(1) Naber, W. J. M.; Faez, S.; van der Wiel, W. G. *J. Phys. D: Appl. Phys.* **2007**, *40*, R205−R228.
(2) Nguyen, T. D.; Hukic-Markosian, G.; Wang, F.; Wojcik, L.; Li, X.; Ehrenfreund, E.; Vardeny, Z. V. *Nat. Mater.* **2010**, *9*, 345−352.
(3) Xiong, Z. H.; Wu, D.; Vardeny, Z. V.; Shi, J. *Nature* **2004**, *427*, 821−824.
(4) Dediu, V.; Hueso, L. E.; Bergenti, I.; Riminucci, A.; Borgatti, F.; Graziosi, P.; Newby, C.; Casoli, F.; De Jong, M. P.; Taliani, C.; Zhan, Y. *Phys. Rev. B* **2008**, *78*, 115203−115209.
(5) Wang, F. J.; Yang, C. G.; Vardeny, Z. V.; Li, X. G. *Phys. Rev. B* **2007**, *75*, 245324−245331.
(6) Dediu, V. A.; Hueso, L. E.; Bergenti, I.; Taliani, C. *Nat. Mater.* **2009**, *8*, 707−716.
(7) Mooser, S.; Cooper, J. F. K.; Banger, K. K.; Wunderlich, J.; Sirringhaus, H. *Phys. Rev. B* **2012**, *85*, 235202−235209.
(8) Wang, S.; Shi, Y. J.; Lin, L.; Chen, B. B.; Yue, F. J.; Du, J.; Ding, H. F.; Zhang, F. M.; Wu, D. *Synth. Met.* **2011**, *161*, 1738−1741.
(9) Chen, B. B.; Zhou, Y.; Wang, S.; Shi, Y. J.; Ding, H. F.; Wu, D. *Appl. Phys. Lett.* **2013**, *103*, 072402-1− 072402-4.
(10) Geim, A. K.; Novoselov, K. S. *Nat. Mater.* **2007**, *6*, 183−191.
(11) Zhang, Y.; Tan, Y. W.; Stormer, H. L.; Kim, P. *Nature* **2005**, *438*, 201−204.
(12) Castro Neto, A. H.; Guinea, F.; Novoselov, K. S.; Geim, A. K. *Rev. Mod. Phys.* **2009**, *81*, 109−162.
(13) Hill, E. W.; Geim, A. K.; Novoselov, K.; Schedin, F.; Blake, P. *IEEE Trans. Magn.* **2006**, *42*, 2694−2696.

(14) Han, W.; Pi, K.; Bao, W.; McCreary, K. M.; Li, Y.; Wang, W. H.; Lau, C. N.; Kawakami, R. K. *Appl. Phys. Lett.* **2009**, *94*, 222109−222112.
(15) Tombros, N.; Jozsa, C.; Popincuic, M.; Jonkman, H. T.; van Wees, B. J. *Nature* **2007**, *448*, 571−575.
(16) Han, W.; Kawakami, R. K. *Phys. Rev. Lett.* **2011**, *107*, 047207−047211.
(17) Liao, Z. M.; Wu, H. C.; Kumar, S.; Duesberg, G. S.; Zhou, Y. B.; Cross, G. L. W.; Shvets, I. V.; Yu, D. P. *Adv. Mater.* **2012**, *24*, 1862−1866.
(18) Banerjee, T.; van der Wiel, W. G.; Jansen, R. *Phys. Rev. B.* **2010**, *81*, 214409−214415.
(19) Mohiuddin, T. M. G.; Hill, E.; Elias, D.; Zhukov, A.; Novoselov, K.; Geim, A. *IEEE Trans. Magn.* **2008**, *44*, 2624−2627.
(20) Cobas, E.; Friedman, A. L.; van't Erve, O. M. J.; Robinson, J. T.; Jonker, B. T. *Nano Lett.* **2012**, *12*, 3000−3004.
(21) Chen, J. J.; Meng, J.; Zhou, Y. B.; Wu, H. C.; Bie, Y. Q.; Liao, Z. M.; Yu, D. P. *Nat. Communs.* **2013**, *4*, 1921−1928.
(22) Iqbal, M. Z.; Iqbal, M. W.; Lee, J. H.; Kim, Y. S.; Chun, S.-H.; Eom, J. *Nano Res.* **2013**, *6*, 373−380.
(23) Meng, J.; Chen, J. J.; Yan, Y.; Yu, D.-P.; Liao, Z.-M. *Nanoscale* **2013**, *5*, 8894−8898.
(24) Ferrari, A. C.; Meyer, J. C.; Scardaci, V.; Casiraghi, C.; Lazzeri, M.; Mauri, F.; Piscanec, S.; Jiang, D.; Novoselov, K. S.; Roth, S.; Geim, A. K. *Phys. Rev. Lett.* **2006**, *97*, 187401−187405.
(25) Ni, Z. H.; Wang, Y. Y.; Yu, T.; Shen, Z. X. *Nano Res.* **2008**, *1*, 273−291.
(26) Sze, S. M.; Ng, K. K. *Physics of Semiconductor Devices*; John Wiley & Sons Inc.: Hoboken, NJ, 2007.
(27) Lu, W. J.; Sun, Y. P.; Zhu, X. B.; Song, W. H.; Du, J. J. *Mater. Lett.* **2006**, *60*, 3207−3211.